Sensors and Actuators B 213 (2015) 295–304

Contents lists available at ScienceDirect

Sensors and Actuators B: Chemical

journal homepage: www.elsevier.com/locate/snb

Affinity based glucose measurement using fiber optic surface plasmon resonance sensor with surface modification by borate polymer

Dachao Li[a,*], Jianwei Wu[a], Peng Wu[a], Yuan Lin[b], Yingjuan Sun[b], Rui Zhu[a], Jia Yang[a], Kexin Xu[a]

[a] State Key Laboratory of Precision Measuring Technology and Instruments, Tianjin University, Tianjin 300072, China
[b] State Key Laboratory of Polymer Physics and Chemistry, Changchun Institute of Applied Chemistry, Chinese Academy of Sciences, Changchun, China

ARTICLE INFO

Article history:
Received 3 November 2014
Received in revised form 21 January 2015
Accepted 10 February 2015
Available online 19 February 2015

Keywords:
Glucose detection
Surface plasmon resonance
Fiber optic sensor
Borate polymer
Surface modification

ABSTRACT

An affinity based method of glucose measurement using a fiber optic surface plasmon resonance (FO-SPR) sensor with surface modification by a borate polymer was proposed. In this method, the sensor is able to obtain the glucose concentration by detecting the surface refractive index of the sensor, which could avoid the impact of bioelectricity from viable tissues when applied for implantable measurement. A biocompatible borate polymer, PAA-ran-PAAPBA, which is capable of associating and dissociating with glucose molecules dynamically, performed non-consumption measurement of glucose, thereby enabling the possibility of glucose detection in hypoglycemic situations. Numerical simulation was performed based on the FO-SPR theory, and an online-transmission FO-SPR sensor with optimized structural parameters was fabricated. PAA-ran-PAAPBA was synthesized and immobilized onto the surface of the FO-SPR sensor using layer-by-layer self-assembly technique. An experimental system was built, and contrast-measurement experiment for 1–10 and 10–300 mg/dL glucose solutions was performed; the FO-SPR sensor bonded with the borate polymer exhibited higher accuracy, especially for low-concentration detection. This study laid a technical foundation for further exploration of implantable measurement systems for blood glucose.

1. Introduction

Diabetes mellitus is a common disease that threatens human health, and it is important to monitor the blood glucose of diabetics continuously for diagnostics and treatment [1–5]. To date, the method for continuous monitoring of blood glucose that has been used in clinical treatment essentially comprises biosensors based on enzyme electrode [6–9], and the most representative products include SEVEN? *R* Plus (DexCom, Inc.) [10], Paradigm? *R* REAL-Time (Medtronic, Inc.) [11] and FreeStyle Navigator? *R* (Abbott Laboratories) [12]. These devices determine the concentration of blood glucose by detecting the glucose molecule in the interstitial fluid (ISF), which is minimally invasive, practical and provides a quick response. However, these implantable biosensors based on enzyme electrode work by detecting the electric current of the glucose oxidation catalyzed by the oxidase immobilized on the sensor. Thus, they are susceptible to the bioelectricity in the viable tissues, which can cause a significant drift in the measuring signal, making them inappropriate for long-term monitoring. The glucose concentration of diabetics provided by these biosensors is always inaccurate, and it is necessary to calibrate them periodically using finger-prick blood extraction, which brings sufferings to the patients. Additionally, the glucose will be consumed irreversibly [13–15] because of the oxidation, resulting in an inaccuracy at low glucose concentration. Consequently, it is almost impossible to find hypoglycemic states in the clinical treatment of diabetes.

The sensing technique based on fiber optic provides an excellent approach to fabricate miniaturized sensors, which enables the possibility of implanting the sensor into subcutaneous tissues. In recent years, the optical glucose sensing is emerging and some fiber optic sensors have been used for glucose detection, such as the fluorescence sensors [16,17] and fiber optic attenuation total reflection (FO-ATR) sensors [18]. Fluorescence sensing is a sophisticated technology, however, the compound that could produce fluorescence effect is limited and the response speed of these sensors is relatively low, which is unsuitable for the continuous monitoring of diabetics. The FO-ATR sensor has a rapid response but the performance of this sensor is positively correlated to the optical length [19]. However, the size of the sensor for implantable measurement restricts the optical length, thus limiting the performance of the sensor. In our

* Corresponding author. Tel.: +86 22 27403916; fax: +86 22 27406726.
E-mail address: dchli@tju.edu.cn (D. Li).

http://dx.doi.org/10.1016/j.snb.2015.02.039
0925-4005/

study, a method of glucose measurement based on fiber optic surface plasmon resonance (FO-SPR) sensor is presented. The sensor measured glucose concentration by detecting the surface refractive index of the interstitial fluid instead of the electric current. Thus, it could avoid the impact of bioelectricity from viable tissues and the signal would be more reliable when applied for implantable measurement.

As the component of the interstitial fluid is complex, any component could cause the variation of the refractive index. Thus, the implantable FO-SPR sensors need to immobilize specific biomolecules that could selectively absorb the glucose to implement the detection. The representative biomolecules are concanavalin (ConA) [20,21] and D-galactose/D-glucose binding protein (GGBP) [22–24]. They have good affinity to the glucose molecules, which have been used to realize the specific measurement of glucose. However, ConA is toxic, and it is easy to trigger immune response. GGBP is nontoxic but difficult to synthesize. Additionally, it is physically and chemically instable. There are also reports showing that boronic acid is a biocompatible group with low cytotoxicity and low immunogenicity, especially for the 3-acrylamidophenylboronic acid (AAPBA) [25–27]. However, the poor solubility limits its application. Recently, Li et al. developed poly(acrylamide-*ran*-3-acrylamidophenylboronic acid) (PAA-PAAPBA), the introduction of biocompatible hydrophilic PAA segments can improve the water solubility, and this copolymer has been used for the glucose detection. The experiment performed by Li et al. also confirmed that this polymer just specifically absorbed glucose molecules, but insusceptible of other compounds or solvents [28]. In this study, the borate polymer, PAA-*ran*-PAAPBA [29], was used for the first time to modify the surface of the FO-SPR sensor and realized the specific measurement of the glucose. The borate polymer was synthesized, and then immobilized onto the surface of the FO-SPR sensor using a layer-by-layer self-assembly technique [30]. The immobilized polymer exists in a solid state on the surface of the sensor and it is able to associate and disassociate with the glucose molecules dynamically. It did not consume glucose and provided a more accurate measurement, which enabled the possibility of glucose detection in the hypoglycemic situations. Compared with conventional SPR sensors modified by ConA and GGBP, the FO-SPR sensor modified by PAA-ran-PAAPBA has excellent stability, remarkable affinity to glucose and high sensitivity. This study established a technical foundation for implantable glucose measurement by FO-SPR sensor in clinical applications.

2. Method of glucose measurement by FO-SPR sensor with affinity based surface modification

2.1. Sensing principle of the FO-SPR sensor

As shown in Fig. 1(a), after a white light source is coupled into the core of fiber optic, it produces internal total reflection with various reflection angles θ, and the evanescent wave is generated [31] simultaneously, the electric field intensity of which decays exponentially at the interface of the core of fiber optic and the metal film. The evanescent wave then excites the collective oscillation of free electrons on the surface of the gold film, generating a surface plasmon wave (SPW). The wave vector of the SPW is given by the following relation:

$$k_{sp} = k_0 \left(\frac{\varepsilon_m \varepsilon_s}{\varepsilon_m + \varepsilon_s} \right)^{1/2} \quad (1)$$

where k_0 is the wave vector of light in free space, ε_m and ε_s are the dielectric constants of the metal and the dielectric medium, respectively. The wave vector of the incident light is given by the following relation

$$k_{fo} = \frac{\omega}{c} \sqrt{\varepsilon_{fo}} \quad (2)$$

where k_{fo} is the wave vector of the incident light in the fiber optic with dielectric constant ε_{fo}, ω the angular frequency and c is the speed of light in free space. When the horizontal component of the incident light wave vector ($k_x = k_{fo} \sin\theta$) is equal to the SPW vector (k_{sp}) at the interface of gold film and glucose solution, or the following relation is satisfied:

$$\frac{\omega}{c} \sqrt{\varepsilon_{fo}} \sin\theta = k_0 \left(\frac{\varepsilon_m \varepsilon_s}{\varepsilon_m + \varepsilon_s} \right)^{1/2} \quad (3)$$

the complete transfer of energy from the incident light to the surface plasmon takes place. This phenomenon is termed as SPR [32].

FO-SPR can be equivalent to the superposition of multiple prism SPR reflection. As the wave vector of the incident light is related to the wavelength, when an incident light at particular wavelength meets the condition of exciting SPR, the total reflection coefficient (reflectivity) of incident light reaches the minimum (shown in Fig. 1(b)) where the wavelength is called the resonance wavelength [33]. It is extremely sensitive to the variation of the optical refractive index on the surface of the gold film. Thus, glucose solutions with various concentrations can be characterized by detecting the refractive index fluctuation and the corresponding resonance wavelengths, which avoids the impact of bioelectricity when used for implantable glucose detection.

2.2. Principle of reaction between boric acid and glucose

In general, the boric acid possesses functional hydroxyl groups that are capable of strongly combining glucose molecules. As shown in Fig. 2(a), boric acid exists in equilibrium between the normal, uncharged state and a dissociative, negatively charged state in an aqueous solution. The reaction of boric acid and glucose is shown in Fig. 2(b): it is a condensation reaction between the hydroxyls of the boric acid and the glucose molecule. When the concentration of the glucose is high, the glucose molecules could be adsorbed by the

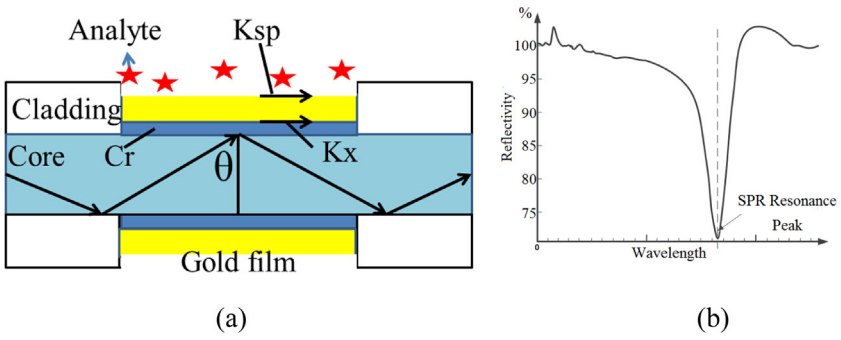

Fig. 1. Sensing principle of FO-SPR sensor.

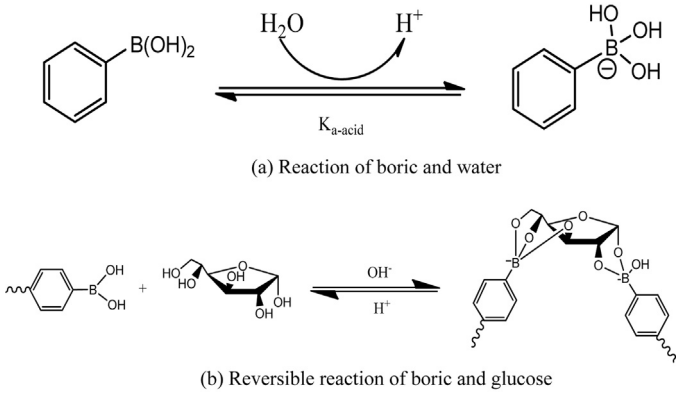

Fig. 2. (a) Reaction of boric and water. (b) Reversible reaction of boric and glucose.

polymer. When the concentration is lower, the glucose molecules would dissociate with the polymer and go back to the aqueous solution. It has been testified by experiment that this reaction is reversible, and it does not consume the glucose [34], which consequently enables the possibility for glucose detection in clinically hypoglycemic situations. Besides, the flexible association and dissociation makes it unnecessary to clean the sensor when it is used for implantable application. Thus, it is very suitable for long-term monitoring of glucose.

3. Structure design and optimization of the FO-SPR sensor

3.1. Theoretical analysis of FO-SPR sensor

Fig. 3 shows the four-layer structure of the FO-SPR sensor. The wavelength and the incident angle of the incident light in the core of fiber is λ and θ, respectively. The total FO-SPR reflection coefficient can be expressed as:

$$r_p(\lambda, \varepsilon_0, \varepsilon_1, \varepsilon_2, \varepsilon_3, d_1, d_2, L) = \left(\frac{1}{m}\right) \sum_{i=1}^{m} r_i^{N_r(L,D,\theta_i)} \times W \quad (4)$$

It is a function of the incident light wavelength, where L is the length of the fiber optic sensing region, D the core diameter of fiber optic, N_r the number of reflection and can be represented as $N_r = L/(D \times \tan\theta)$ and m is the number of propagation mode (i.e. the incident angle number within a certain range of discrete values), which is better as a larger value. W is the mode density distribution function, corresponding to the energy distribution of the various propagation modes in the fiber, and can be represented as:

$$W = \frac{(18,510 + 369.4 \times (90 - \theta_i) - 1071 \times (90 - \theta_i)^2 + 133 \times (90 - \theta_i)^3 - 4.754 \times (90 - \theta_i)^4))}{100,000} \quad (5)$$

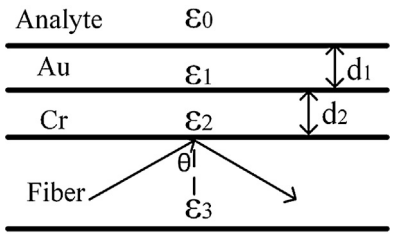

Fig. 3. The four-layer FO-SPR structure.

r_i is the reflectivity of single beam light and can be obtained according to the Fresnel formulas:

$$r_i = \left| \frac{r_{23} + r_{012} e^{-2\alpha_2 d_2}}{1 + r_{23} + r_{012} e^{-2\alpha_2 d_2}} \right|^2 \quad (6)$$

where:

$$r_{012} = \frac{r_{12} + r_{01} e^{-2\alpha_1 d_1}}{1 + r_{12} + r_{01} e^{-2\alpha_1 d_1}}, \quad r_{01} = \frac{\varepsilon_0\alpha_1 - \varepsilon_0\alpha_1}{\varepsilon_0\alpha_1 - \varepsilon_0\alpha_1},$$
$$r_{12} = \frac{\varepsilon_1\alpha_2 - \varepsilon_2\alpha_1}{\varepsilon_1\alpha_2 - \varepsilon_2\alpha_1}, \quad r_{23} = \frac{\varepsilon_2\alpha_3 - \varepsilon_3\alpha_2}{\varepsilon_2\alpha_3 - \varepsilon_3\alpha_2} \quad (7)$$

$$\alpha_i = (\beta^2 - k_0^2 \varepsilon_i)^{1/2} (i = 0,\ 1,\ 2,\ 3) \quad (8)$$

$$\beta = k_0 \sqrt{\varepsilon_3 \sin\theta} \quad (9)$$

$$k_0 = \frac{2\pi}{\lambda} \quad (10)$$

r_{01}, r_{12}, r_{23} are the reflectivity at the interface of the glucose solution and the gold film, the interface of the chromium film and the gold film, the interface of chromium film and core of fiber optic, respectively. d_1 and d_2 is the thickness of the gold film and the chromium film. k_0 is the wave vector in a vacuum. ε_0, ε_1, ε_2, ε_3 are the permittivity of the glucose solution, gold film, chromium film and the core of fiber optic, respectively, which are also the function of the incident wavelength. As the incident angle of the light can be controlled in the light source, the total reflectivity of the SPR is only correlated to the wavelength of the incident light.

In order to optimize the structure of the FO-SPR sensor and improve its performance, numerical simulations based on the FO-SPR theory were performed here, including the core diameter of the fiber optic D, the length of the sensing region L, the thickness of the gold layer d_1 and the chromium layer d_2. The reflectivity and sensitivity (wavelength shift when the refractive index changed) depending on these parameters is simulated here. For the spectra analysis of a higher accuracy and sensitivity, the spectra should have a larger attenuation depth as well as a smaller full width half maximum (FWHM). Here, the sensitivity of the sensor is defined as the shift of the resonance wavelength when the refractive index changed by unit. Keeping the other structural parameters constant, the shift of the resonance wavelength could be calculated by changing the refractive index.

3.2. Structural optimization of FO-SPR sensor

In the simulation, shown in Fig. 4(a1), when the core diameter increases from 125 to 600 μm, the reflectivity and attenuation depth of the SPR curve increases, whereas the FWHM decreases, and the resonance wavelength is almost unchanged. Additionally, Fig. 4(a2) shows that with increased core diameter, the sensitivity increases gradually. In addition, it is unnecessary for special customization when the core diameter is 600 μm. Based on the considerations of spectral-analysis accuracy and production cost, the core diameter 600 μm is selected. In Fig. 4(b1), as the length of the sensing region increases, the reflectivity decreases, and the attenuation depth of the SPR curve increases while the sensitivity is decreasing, as shown Fig. 4(b2). To balance the accuracy and sensitivity, 15 mm is selected for the length of sensing region. In Fig. 4(c1) and (c2), the thickness of chromium layer has almost no impact on the attenuation depth and the sensitivity. In Fig. 4(d1), as the thickness of the gold film increases, the SPR curve has a red shift and the

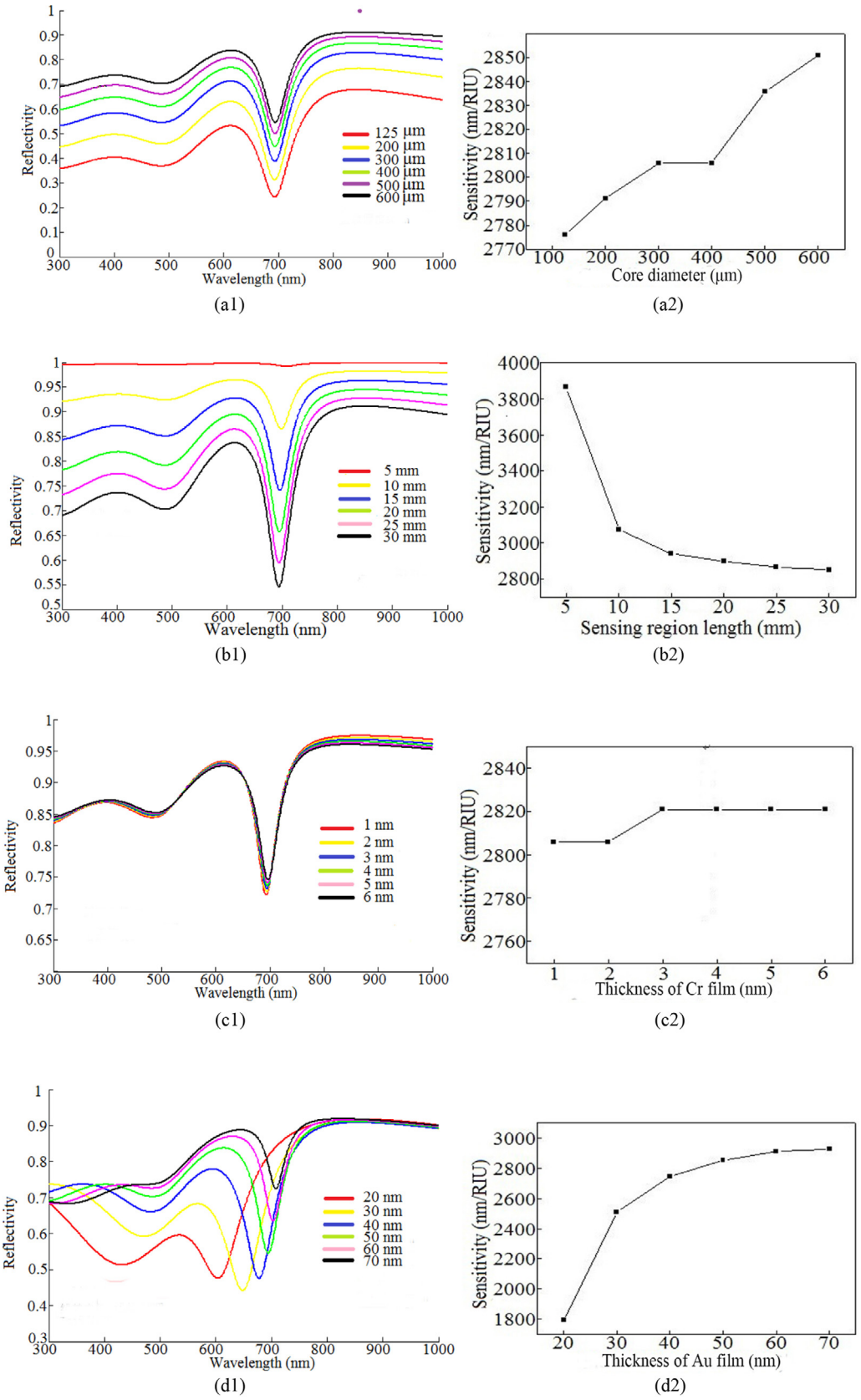

Fig. 4. Numerical simulation of the relationship between the sensor performance and its structural parameters, including the core diameter of fiber optic ((a1) and (a2)), the length of sensing region ((b1) and (b2)), the thickness of the Cr film ((c1) and (c2)) and the Au film ((d1) and (d2)).

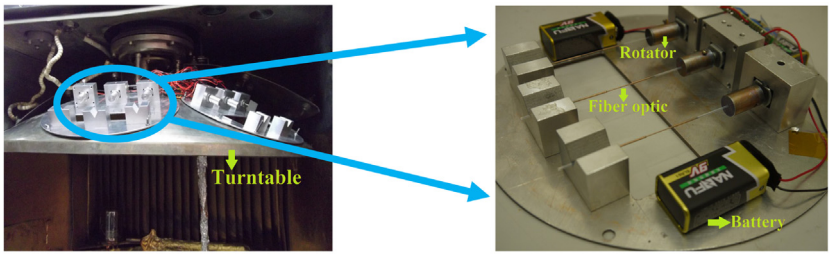

(a) The revolution turntable of the metal deposition system (b) The rotator for fiber optic rotating

Fig. 5. The revolving turntable of the deposition system and the mounting device for fiber optic rotating.

sensitivity increases (Fig. 4(d2)), meanwhile the attenuation depth and FWHM decreases. Thus, to enhance the spectral-analysis accuracy and to control the film thickness accurately in manufacture, the optimal parameters of chromium layer and gold film thickness are 5, 50 nm, respectively.

4. Fabrication of the FO-SPR sensor and its affinity based surface modification

4.1. The fabrication of FO-SPR sensor

A multimode fiber with a core diameter of 600 μm was utilized to fabricate an online-transmission FO-SPR sensor. The fabrication process of the FO-SPR sensor includes pretreatment of the fiber optic, vacuum coating of the circumferential surface of the fiber core with a 5 nm chromium layer and a 50 nm gold film to form the sensing region. The coating layer and the cladding of 15 mm length were stripped in the middle of the fiber optic using physical methods, followed by an alcohol ultrasonication for cleaning the delcadding portion. After that, chromium layer and gold film with a thickness of 5 and 50 nm, respectively, were deposited on the circumferential surface of this portion via a vacuum deposition system (ZZS700-2/G, Nanguang, China). Fig. 5(a) shows turntable of the deposition system, the substrates could be mounted on the top of the turntable, and the turntable could revolve so that the metal particles evaporated from the bottom of the system could be deposited onto the bottom side of the substrates. However, this commercial system is just suitable for the metal deposition on flat substrates but not for cylinders, because the upper half section is beyond the deposition range.

Here, we focus on the need of depositing a uniform and homogeneous metal layer on the circumferential surface of the fiber optic. To overcome the defect of this commercial system, a novel metal deposition method combining the turntable revolving and the fiber optic rotating was brought forward. The fiber optic was mounted to a rotator, as shown in Fig. 5(b). With the clamped rotator rotating and the turntable revolving simultaneously, the metal particles evaporated from the bottom of the deposition system could be deposited uniformly to the cylinder of the fiber optic. Here, the chromium layer was used only for enhancing the adhesion between the gold and the surface of fiber optic. After metal deposition, an SMA905 connector was installed on both sides of the fiber optic to couple the light. Fig. 6 shows the FO-SPR sensor fabricated.

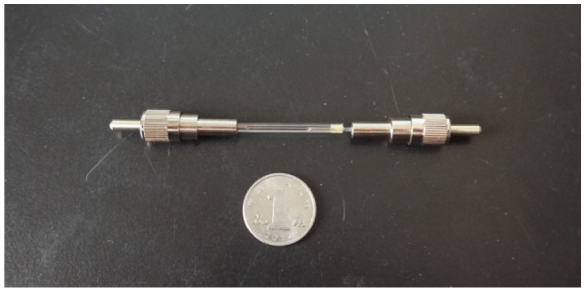

Fig. 6. The fabricated SPR sensor.

4.2. Synthesis of borate polymer

4.2.1. Synthesis of monomer AAPBA

3-Aminophenylboronic acid (5 g, 36.5 mmol, Sigma Aldrich) was dissolved in NaOH solution (2 M, 73 mL, 146 mmol) at 0 °C, and then cold acryloyl chloride (5.9 mL, 7 mmol, Sigma Aldrich) was added dropwise to the vigorously stirred mixture over 15 min [28]. HCl solution (1 M) was slowly added to the reaction mixture until the pH reached 1.0. Next, the white solids that precipitated were filtered and washed with cold water. Then, the filtrate was extracted with EtOAc three times. The organic phase was washed with brine and evaporated to give off-white solids, which were combined with the above precipitates. Finally, recrystallization in H_2O produced off-white AAPBA crystals, the monomer AAPBA is shown in Fig. 7. To characterize the AAPBA, the ^1H and ^{13}C NMR spectra were recorded on a Mercury VX-300 spectrometer. ^1H (300 MHz, DMSO-d_6): δ 10.06 (s, 1H), 8.01 (s, 2H), 7.87 (s, 2H), 7.81 (d, J = 8.1 Hz, 1H), 7.49 (d, J = 7.2 Hz, 1H), 7.27 (t, J_1 = 7.5 Hz, J_2 = 7.8 Hz, 1H), 6.44 (dd, J_1 = 16.8 Hz, J_2 = 9.9 Hz, 1H), 6.23 (dd, J_1 = 17.1 Hz, J_2 = 2.1 Hz, 1H), 5.72 (dd, J_1 = 9.9 Hz, J_2 = 2.1 Hz, 1H). ^{13}C NMR (75.5 MHz, DMSO-d_6): δ 163.8, 138.8, 135.6, 132.7, 130.0, 128.4, 127.3, 126.0, 122.0.

4.2.2. Synthesis of PAA-ran-PAAPBA

Polymerization: acrylamide (3.72 g, 52.4 mmol), AAPBA (0.20 g, 2 mmol), and AIBN (21.5 mg, 0.13 mmol) were dissolved in DMSO. The mixture was bubbled with nitrogen for half an hour and subjected to a 70 °C oil bath for 24 h. After it was cooled to room temperature, the gel was subjected to dialysis against ultrapure water for 24 h. The aqueous phase was precipitated by acetone and dried in vacuum oven at 50 °C to give 3.07 g white solids, as shown in Fig. 8.

4.3. Immobilization procedure of borate polymer

In this paper the borate polymer was immobilized onto the gold surface by the layer-by-layer self-assembly technique. Layer-by-layer technique [30] is an alternative deposition method using

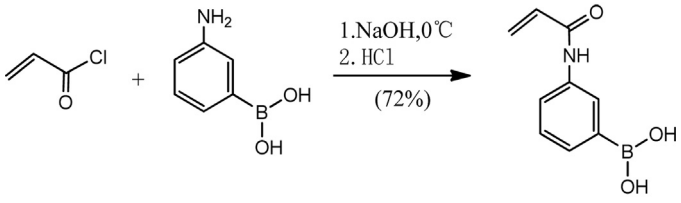

Fig. 7. Synthesis of borate monomer.

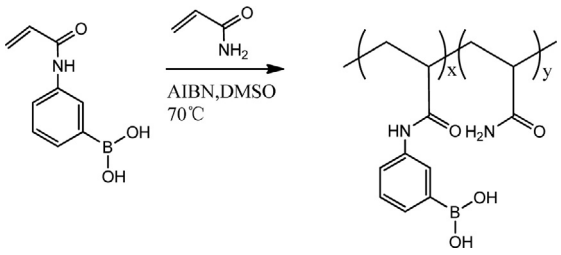

Fig. 8. Synthesis of borate polymer.

weak interactions (electrostatic attraction between ions, hydrogen bond, etc.) as driving force to construct a multilayer film, which has the advantages of simple process, free from size, shape and type of the substrate. The PAA segments could provide the positive charges for the layer-by-layer method in this study. The detailed process is as follows, and the schematic diagram of the immobilization is shown in Fig. 9.

4.3.1. Pretreatment of FO-SPR sensor

The SPR sensor was immersed in a solution (1:1:5 mixture of ammonia, H_2O_2 and H_2O) at 75 °C for 15 min, followed by rinsing with plenty of ultrapure water and drying with a nitrogen stream, after which it was prepared for assembly.

4.4. Reagents

The dipping concentration of polyelectrolytes was 1 mg/mL for poly(diallyldimethylammonium chloride) (PDDA) (M_W = ~200,000–350,000, Sigma Aldrich) and poly(sodium 4-styrene sulfonate) (PSS) (M_W = 70,000, Sigma Aldrich), including 0.25 M NaCl each. The solvent used to dissolve polyelectrolyte was deionized water, which was purified using a UNIQUE-R20 system (18.2 MΩ). PDDA and PSS solutions were prepared by dissolving the corresponding materials in deionized water, and the final concentrations were both 1 mg/mL containing 0.25 M NaCl. The borate polymer was solved in 0.01 M NaH_2PO_4 solution (pH 4.85), and the final concentration was 0.1 mg/dL, including 0.25 M NaCl.

4.5. Assembly

(a) The gold film of the sensor was first dipped into the PDDA solution for 10 min, and then it was rinsed with ultrapure water to remove excess polycations and dried with nitrogen. The PDDA is immobilized onto the surface of the gold film by the covalent bond between the N-functional group and the gold. (b) The gold film with the positive charged surface was subsequently dipped into the PSS solution for 10 min, followed by rinsing with ultrapure water and drying with nitrogen as above. Steps (a) and (b) were repeated until 2.5 bilayers $(PDDA/PSS)_2PDDA$ with the PDDA as the outmost surface were obtained, which served as precursor film. Each bilayer repeat unit consisting of one polycation layer and one polyanion layer and number 2 means the times of cycle. The precursor multilayer film provides uniform positive charge and smooth surface for subsequent deposition. (c) The gold substrate with precursor film was dipped into the PSS solution for 30 min and rinsed with ultrapure water and dried with nitrogen. (d) Subsequently, the gold substrate was dipped into the PAA-ran-PAAPBA solution for 30 min, the PAA-ran-PAAPBA carries positive charge because of protonated amino groups, and then it was rinsed with ultrapure water and dried with nitrogen. Steps (c) and (d) were repeated twice, and 2 bilayers $(PSS/PAA\text{-}ran\text{-}PAAPBA)_2$ were assembled and two cycles can guarantee the PAA-ran-PAAPBA can cover the substrate completely for the glucose test.

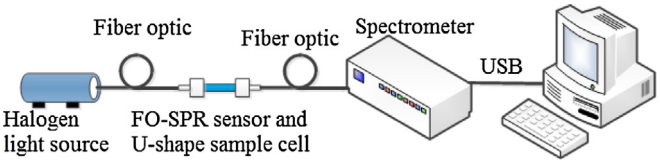

Fig. 10. Schematic diagram of the experimental system for glucose detection.

5. Experiment and discussion

The normal blood-glucose concentration in the fasting state is approximately 60–110 mg/dL, which will increase to 140 mg/dL after a meal but always below 200 mg/dL. Thus, the measurement range of glucose concentration here is 10–300 mg/dL. To further evaluate the FO-SPR sensor and explore the LOD (limit of detection) of it, glucose solutions of 1–10 mg/dL is also measured.

5.1. Experimental system for glucose detection

The schematic diagram of the measuring system is shown in Fig. 10. The light emitted from the halogen light source (Ocean Optics, HL-2000) was coupled into a UV–vis fiber optic (core diameter 600 μm, Ocean Optics) and propagated to the FO-SPR sensor placed in the U-shape example cell through the SMA905 connector. The output spectrum was detected by a spectrometer (Ocean Optics, USB2000) and then transferred to computer for data analysis.

Additionally, if the sensor is implanted subcutaneously, only the sensing area of the FO-SPR sensor will be implanted, while other electronic devices referred above will implement the measurement out of body. As the sensor detects the variation of refractive index around the sensor and exports the attenuated spectrum, it effectively avoids the impact of bioelectricity of human body.

5.2. Resonance peak calculation by weighted centroid method

Savitzky–Golay filtering is used to eliminate certain data elements that with high deviations and smooth the data directly in the time domain prior to calculating the resonance wavelength. The noises contained in the spectrum hindered the accurate determination of the lowest point in the resonance curve. To overcome this issue, a weighted centroid method [35] was used to analyze the SPR spectrum, shown in Fig. 11. The baseline was set in the SPR curves to ensure that the number of pixels below each baseline was a fixed value. Only pixels below the baseline were used for the

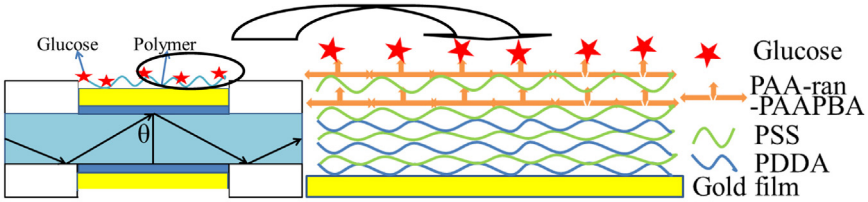

Fig. 9. Schematic diagram of borate polymer immobilization.

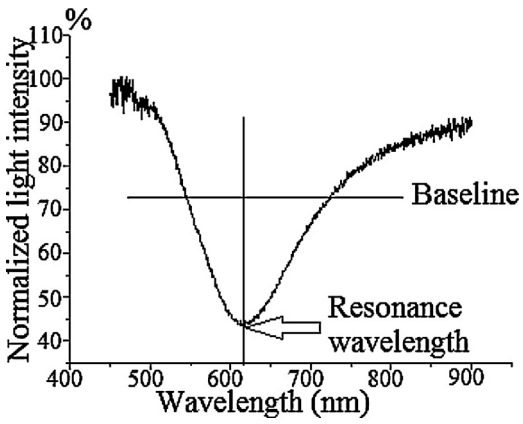

Fig. 11. Diagram of the weighted centroid method.

calculation and analysis. The weighted centroid method aimed to take the distance between each pixel and the baseline as weighting so that the contribution of centroid-position calculation made by the pixels near the baseline could be increased. This method reduced the deviation from the basic shape changing of the curve. Here, the usability of common n-th order curve-fitting was also considered. However, as the SPR spectrum is asymmetric, it is inappropriate to fit the curve using 2-th (quadratic) fitting. 3-th (cubic) polynomial has zero or two extreme points, while hopefully, we want to obtain only one extreme point from the output spectrum. Thus, 3-th (cubic) fitting is also inappropriate. The fitting curve will become more complicated when n is equal to or larger than 4. Taking all these into consideration, the weighted centroid method was chosen eventually. The centroid position can be expressed as:

$$R = \frac{\sum_i [\omega_i (L - I_i) x_i]}{\sum_i [\omega_i (L - I_i)]} \tag{11}$$

where L is the value of baseline, x_i the normalized intensity of pixel i, x_i the abscissa of pixel i, and $\omega_i = L - I_i$ is the weighting of pixel i.

5.3. Glucose measurement

5.3.1. Measuring experiment for 1–10 mg/dL glucose solutions

Using the FO-SPR sensor immobilized polymer and without polymer, respectively, glucose solutions (1–10 mg/dL, increment of 1 mg/dL) were sequentially injected to the U-shape sample cell. The resulting spectrum for different sensors is shown in Fig. 12(a). Based on the data obtained from the spectrums, the resonance wavelengths of different concentrations were calculated by weighted centroid method. Then these corresponding resonance wavelengths were fitted versus the glucose concentrations by quadratic curve, and the result is shown in Fig. 12(b). The R-squared of the curve for sensors with and without polymer is 0.990 and 0.673, respectively.

5.3.2. Measuring experiment for 10–300 mg/dL glucose solutions

Using the FO-SPR sensor immobilized polymer and without polymer, respectively, 10–300 mg/dL glucose solutions were also measured with a concentration increment of 10 mg/dL. The resulting spectrum (for 10–300 mg/dL) is shown in Fig. 13(a). The corresponding resonance wavelengths obtained from weighted centroid method were fitted versus glucose concentrations by quadratic curve. The fitting curve is shown in Fig. 13(b), and the R-squared of the curve for sensors with and without polymer is 0.978 and 0.785, respectively.

6. Discussion

It could be concluded from Figs. 12(a) and 13(a) that the resonance wavelength of the FO-SPR sensor has a red shift with the concentration of glucose increasing, which indicated that the surface refractive index of the sensor has changed.

In the measurement of low concentrations (1–10 mg/dL), shown in Fig. 12(a), the spectrums of the FO-SPR sensor immobilized borate polymer have a relatively larger attenuation depth and the result has higher accuracy, as the R-square of the fitting curve is 0.99, shown in Fig. 12-(b). Besides, the result has good repeatability. However, the sensor without surface modification has a smaller FWHM, meaning that this sensor has higher measurement sensitivity, shown in Fig. 12(b). The low sensitivity exhibited by the modified sensor has been thoroughly discussed, and we think that as the FO-SPR sensor detects the variation of surface refractive index induced by the adsorption of the glucose molecules to the polymer, when the glucose concentration is in 1–10 mg/dL, maybe few glucose molecules could be absorbed by the polymer and the quantity of the glucose molecules has almost no significant change between two single-measurement, resulting the low sensitivity. Additionally, the high sensitivity of the untreated sensor shown in Fig. 12 does not mean the untreated sensor is reliably sensitive, as the repeatability of the result is sometimes unsatisfactory. Wang et al. [36] have demonstrated in their study that the limit of detection (LOD) for glucose in DI water is 0.02 mg/mL. Here, the SPR sensor modified by borate polymer responded accurately in the measurement of glucose solutions with a concentration increment

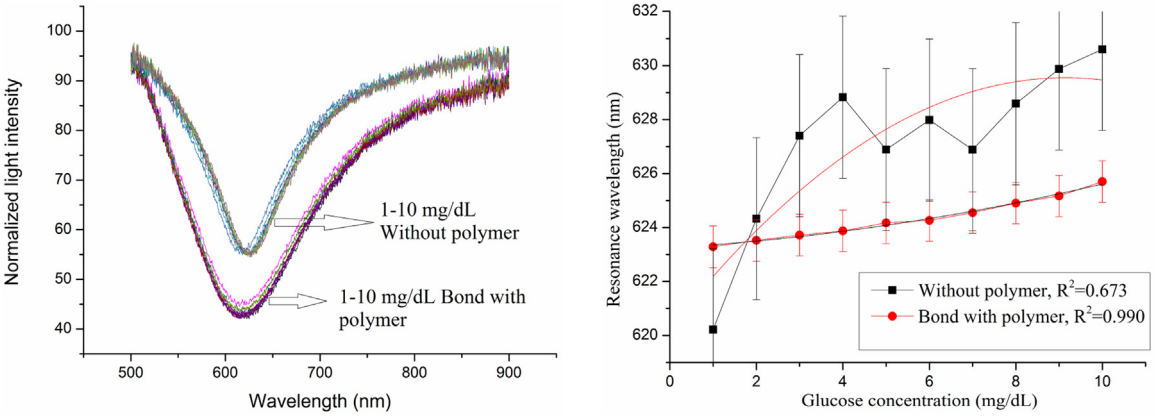

(a) The output spectrum (b) The fitting curve

Fig. 12. The measuring result of 1–10 mg/dL glucose solutions using FO-SPR sensor with and without polymer modification, respectively.

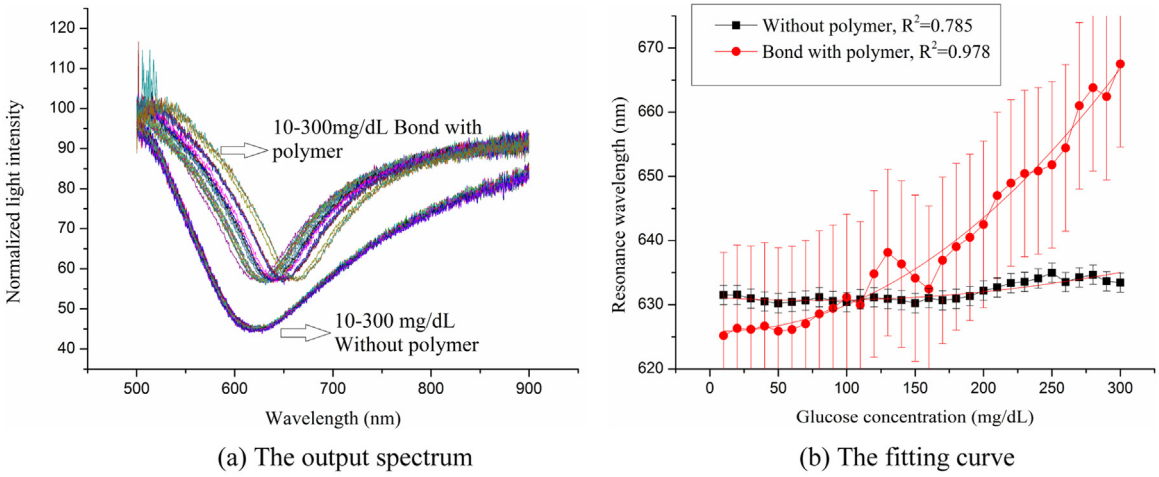

Fig. 13. The measuring result of 10–300 mg/dL glucose solutions using FO-SPR sensor with and without polymer modification, respectively.

of 1 mg/dL (0.01 mg/mL), meaning that it is suitable for low concentration detections, which is beneficial for its application in the clinical treatment of diabetics in hypoglycemic state.

In the measurement of higher concentrations (10–300 mg/dL), the measuring result of FO-SPR sensors with different treatment were compared, shown in Fig. 13(a). The untreated sensor exhibited larger attenuation depth in the measurement, but the spectrums of this sensor have a bigger FWHM as well, meaning it is less sensitive in the measurement of this concentration gradient, which is also confirmed by Fig. 13(b). Additionally, the accuracy of this untreated sensor is also unsatisfactory, shown in Fig. 13(b), the R-square of the fitting curve is just 0.785. After the surface modification using borate polymer, the sensor exhibited higher accuracy and sensitivity in the measurement of high concentrations, the resonance wavelengths increased from 625.2 to 667.5 nm in this concentration gradient, and the R-square of the fitting curve is 0.978. In our anticipation, the sensor modified by borate polymer should be more sensitive in both the low and high concentrations than the untreated sensor. However, this anticipation was just verified by the measuring result of high concentrations. Despite a higher accuracy, the modified sensor did not perform so sensitively for the measurement of low concentrations, this problem might be solved by controlling the layers of the polymer, and would be further explored in the future work.

7. Conclusion

An affinity based method of glucose measurement using FO-SPR sensor was presented. The sensor here detected glucose through measuring the surface refractive index, thus, it is immune to the bioelectricity when implanted subcutaneously. A borate polymer, PAA-ran-PAAPBA, which was able to associate and dissociate with glucose dynamically, was used and achieved non-consumption measurement of glucose, enabling the possibility of glucose detection for diabetics in hypoglycemic state. Numerical simulation was performed according to the theoretical analysis and the FO-SPR sensor with optimized structural parameters was fabricated. The borate polymer was synthesized and immobilized onto the surface of the FO-SPR sensor by layer-by-layer assembly technique. The experimental system for glucose measurement was set up and glucose solutions of 1–10 and 10–300 mg/dL were measured with naked and polymer modified FO-SPR sensor respectively. The modified sensor exhibited higher accuracy, especially for the lower concentrations. Consequently, future studies will further investigate biocompatible encapsulation of the FO-SPR sensor using biological materials and animal experiment.

Acknowledgments

This work was supported by the National Natural Science Foundation of China (No. 61176107, No. 51350110233, No. 11204210, No. 61428402 and No. 61201039), the Key Projects in the Science &Technology Pillar Program of Tianjin (No. 11ZCKFSY01500), the National Key Projects in Non-profit Industry (No. GYHY200906037), and the National High Technology Research and Development Program of China (No. 2012AA022602).

References

[1] P.J. Stout, J.R. Racchini, M.E. Hilgers, A novel approach to mitigating the physiological lag between blood and interstitial fluid glucose measurement, Diabetes Technol. Ther. 6 (2004) 635–644.
[2] C. Zecchin, A. Facchinetti, G. Sparacino, G.D. Nicolao, C. Cobelli, A new neural network approach for short-term glucose prediction using continuous glucose monitoring time-series and meal information, Conf. Proc. IEEE Eng. Med. Biol. Soc. 565 (2011) 5653–5656.
[3] T. Karacolar, A.Z. Hood, E. Topsakal, Design of a dual-band implantable antenna and development of skin mimicking gels for continuous glucose monitoring, Microwave Theory Tech. 56 (2008) 1001–1008.
[4] M. Zanon, M. Riz, G. Sparacino, A. Facchinetti, R.E. Sufi, M.S. Talary, C. Cobelli, Assessment of linear regression techniques for modeling multisensory data for non-invasive continuous glucose monitoring, Conf. Proc. IEEE Eng. Med. Biol. Soc. (2011) 2538–2541.
[5] Y.J. Lee, J.D. Kim, J.Y. Park, Flexible enzyme free glucose micro-sensor for continuous monitoring applications, Conf. Proc. Solid-State Sensors Actuator Microsyst. (2009) 1806–1809.
[6] D.A. Gough, T. Bremer, Immobilized glucose oxidase in implantable glucose sensor technology, Diabetes Technol. Ther. 2 (2000) 377–380.
[7] J. Zhu, Z. Zhu, Z. Lai, R. Wang, X. Guo, X. Wu, G. Zhang, Z. Zhang, Y. Wang, Z. Chen, Planar amperometric glucose sensor based on glucose oxidase immobilized by chitosan film on Prussian blue layer, Sensor 2 (2002) 127–136.
[8] J. Okuda, J. Wakai, N. Yuhashi, K. Sode, Glucose enzyme electrode using cytochrome b(562) as an electron mediator, Biosens. Bioelectron. 18 (2003) 699–704.
[9] J. Wang, Electrochemical glucose biosensors, Chem. Rev. 108 (2008) 814–825.
[10] H.C. Zisser, T.S. Bailey, S. Schwartz, R.E. Ratner, J. Wise, Accuracy of the SEVEN continuous glucose monitoring system: comparison with frequently sampled venous glucose measurements, Diabetes Sci. Technol. 3 (2009) 1149–1154.
[11] D. Deiss, J. Bolinder, J.P. Riveline, T. Battelino, E. Bosi, N. Tubiana-Rufi, D. Kerr, M. Phillip, Improved glycemic control in poorly controlled patients with type 1 diabetes using real-time continuous glucose monitoring, Diabetes Care 29 (2006) 2730–2732.
[12] S. Weinzimer, D. Xing, M. Tansey, R. Fiallo-Scharer, N. Mauras, T. Wysochi, R. Beck, W. Tamborlane, K. Ruedy, Prolonged use of continuous glucose monitors in children with type 1 diabetes on continuous subcutaneous insulin infusion or intensive multiple-daily injection therapy, Pediatr. Diabetes 10 (2009) 91–96.
[13] J. Mastrototaro, J. Shin, A. Marcus, G. Sulur, The accuracy and efficacy of real-time continuous glucose monitoring sensor in patients with type 1 diabetes, Diabetes Technol. Ther. 10 (2008) 385–390.

[14] R.L. Weinstein, S.L. Schwartz, R.L. Brazg, J.R. Bugler, T.A. Peyser, G.V. McGarraugh, Accuracy of the 5-day FreeStyle Navigator continuous glucose monitoring system: comparison with frequent laboratory reference measurements, Diabetes Care 30 (2007) 1125–1130.
[15] D.M. Wilson, R.W. Beck, W.V. Tamborlane, M.J. Dontchev, C. Kollman, P. Chase, L.A. Fox, K.J. Ruedy, E. Tsalikian, S.A. Weinzimer, The accuracy of the FreeStyle Navigator continuous glucose monitoring system in children with type 1 diabetes, Diabetes Care 30 (2007) 59–64.
[16] D.C. Klonoff, Overview of fluorescence glucose sensing: a technology with a bright future, Diabetes Sci. Technol. 6 (2012) 1242–1250.
[17] Y.J. Heo, H. Shibata, T. Okitsu, T. Kawanishi, S. Takeuchi, Long-term in vivo glucose monitoring using fluorescent hydrogel fibers, Conf. Proc. Natl. Acad. Sci. U.S.A. 1104954108 (2011) 1–5.
[18] S. Yu, D. Li, H. Chong, C. Sun, K. Xu, In vitro glucose measurement using tunable mid-infrared laser spectroscopy combined with fiber-optic sensor, Biomed. Opt. Express 5 (2014) 275–286.
[19] L.A. Averett, P.R. Griffiths, K. Nishikida, Effective path length in attenuated total reflection spectroscopy, Anal. Chem. 80 (2008) 3045–3049.
[20] J.C. Pickup, F. Hussain, N.D. Evans, O.J. Rolinski, D.J.S. Birch, Fluorescence-based glucose sensors, Biosens. Bioelectron. 20 (2005) 2555–2565.
[21] R. Ballerstadt, J.S. Schultz, A fluorescence affinity hollow fiber sensor for continuous transdermal glucose monitoring, Anal. Chem. 72 (2000) 4185–4192.
[22] H.V. Hsieh, Z.A. Pfeiffer, T.J. Amiss, D.B. Sherman, J.B. Pitner, Direct detection of glucose by surface plasmon resonance with bacterial glucose/galactose-binding protein, Biosens. Bioelectron. 19 (2004) 653–660.
[23] A. Sakaguchi-Mikami, A. Taniguchi, K. Sode, T. Yamazaki, Construction of a novel glucose-sensing molecule based on a substrate-binding protein for intracellular sensing, Biotech. Bioeng. 108 (2011) 725–733.
[24] K. Weidemaier, A. Lastovich, S. Keith, J.B. Pitner, M. Sistare, R. Jacobson, D. Kurisko, Multi-day pre-clinical demonstration of glucose/galactose binding protein-based fiber optic sensor, Biosens. Bioelectron. 26 (2011) 4117–4123.
[25] X. Wang, X. Zhen, J. Wang, J. Zhang, W. Wu, X. Jiang, Doxorubicin delivery to 3D multicellular spheroids and tumors based on boronic acid-rich chitosan nanoparticles, Biomaterials 34 (2013) 4667–4679.
[26] X. Zhang, S. Lu, C. Gao, C. Chen, X. Zhang, M. Liu, Highly stable and degradable multifunctional microgel for self-regulated insulin delivery under physiological conditions, Nanoscale 5 (2013) 6498–6506.
[27] C. Zheng, Q. Guo, Z. Wu, L. Sun, Z. Zhang, C. Li, X. Zhang, Amphiphilic glycopolymer nanoparticles as vehicles for nasal delivery of peptides and proteins, Pharm. Sci. 49 (2013) 474–482.
[28] S. Li, E.N. Davis, J. Anderson, Q. Lin, Q. Wang, Development of boronic acid grafted random copolymer sensing fluid for continuous glucose monitoring, Biomacromolecules 10 (2009) 113–118.
[29] S. Li, E.N. Davis, J. Anderson, Q. Lin, Q. Wang, Development of boronic acid grafted random copolymer sensing fluid for continuous glucose monitoring, Biomacromolecules 10 (2008) 113–118.
[30] R.M. Iost, F.N. Crespilho, Layer-by-layer self-assembly and electrochemistry: applications in biosensing and bioelectronics, Biosen. Bioelectron. 31 (2012) 1–10.
[31] B. Lee, S. Roh, J. Park, Curent status of micro-and nano-structured optical fiber sensors, Opt. Fiber Technol. 15 (2009) 209–221.
[32] S.K. Srivastava, B.D. Gupta, Simulation of a localized surface-plasmon-resonance-based fiber optic temperature sensor, JOSA A 27 (2010) 1743–1749.
[33] B.D. Gupta, R.K. Verma, Surface plasmon resonance based fiber optic sensors: Principle, probe designs and some applications, Sensors 209 (2009) 1–12.
[34] X. Huang, S. Li, J.S. Schultz, Q. Wang, Q. Lin, A MEMS affinity glucose sensor using a biocompatible glucose-responsive polymer, Sens. Actuators B: Chem. 140 (2009) 603–609.
[35] G.G. Nenninger, M. Piliarik, J. Homola, Data analysis for optical sensors based on spectroscopy of surface plasmons, Meas. Sci. Technol. 13 (2002) 2038–2046.
[36] J. Wang, S. Banerji, N. Menegazzo, W. Peng, Q. Zou, K.S. Booksh, Glucose detection with surface plasmon resonance spectroscopy and molecularly imprinted hydrogel coatings, Talanta 86 (2011) 1233–2141.

Biographies

Dachao Li was born in Nanyang, Henan Province in China in 1976. He received the B.S. degree in Precision Instrument from Tianjin University, Tianjin, China, in 1998 and the M.S. and Ph.D. degrees in Precision Instrument and Mechanics from Tianjin University, Tianjin, China, in 2001 and 2004, respectively. From 2004 to 2006, he did postdoctoral research at Institute of Microelectronics, Peking University, Beijing, China. From 2006 to 2008, he was a research associate at Department of Electrical Engineering and Computer Science, Case Western Reserve University, Cleveland, USA. Presently, he is an associate professor and Ph.D. supervisor in College of Precision Instrument and Optoelectronics Engineering, Tianjin University. His research specializations focus on micro sensor and optofluidics. He has received 15 research projects in PI capacity. He has published more than 60 research articles in international journals, book chapters and conference proceedings. He holds 2 US and Japan patents and 10 Chinese patents. He has been the members of Chinese Society of Micro-Nano Technology and China Instrument and Control Society since 2008. He was a recipient of the New Century Excellent Talents Award from Chinese Ministry of Education in 2013.

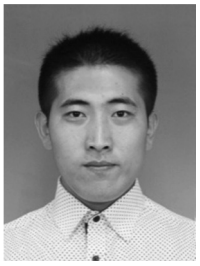

Jianwei Wu received the B.S. degree in electronic information technology and instruments, Zhejiang University of China, Hangzhou, China, in 2012. He is currently pursuing the M.S. degree in precision instrument and optoelectronics engineering at Tianjin University, Tianjin, China. His research interest is fiber optic sensors research based on Surface Plasmon Resonance technology

Peng Wu received the B.S. in instrument science and technology from Tianjin University in 2007, and he received the Ph.D. degree in the same major in 2013. He is currently working in the KLA-Tencor Semiconductor Equipment Technology Company. During his Ph.D. period, his research interest includes the novel optic-fiber sensors research based on Surface Plasmon Resonance technology and the development of portable minimally invasive glucose detection instrument based on SPR biosensor.

Yuan Lin received her B.S. and Ph.D. degree in materials science and engineering from Jilin University, Changchun, China, in 2003 and 2008. From 2006 to 2007, she studied in the Department of Food Science, Rutgers University, USA as a joint Ph.D. student. From 2008 to 2010, she did post-doctoral research at Department of Chemistry and Biochemistry, University of South Carolina, USA. Presently, she is an associate professor in State Key Lab of Polymer Physics and Chemistry, Changchun Institute of Applied Chemistry, Changchun, China. Her research interest includes the design functional biomaterials and the interaction between cell and substrate

Yingjuan Sun received her bachelor degree in polymer material and engineering from Anhui University, Hefei, China, in 2012. From 2012 to now, she studied in the State Key Laboratory of Polymer Physics and Chemistry, Changchun Institute of Applied Chemistry, Changchun, China, as a Ph.D. candidate in Qian Wang's group. Her research focus is mainly on studying the self-assembling conductive polymer patterns with ordered topography and electrical stimulation for the directional growth of neural cells

Rui Zhu received the B.S. degree in measurement and control technology and instrument from Hebei University, Baoding, China, in 2010, and M.S. degree in instrument science and technology from Tianjin University, Tianjin, China, in 2013. He is currently working in Jinhang Institute of Computing Technology, Tianjin, China. During his M.S. period, his research interest includes the research and application on fiber-optic surface plasmon resonance.

Jia Yang received the B.S. degree in measurement and control technology and instrument specialty from Hebei University of Technology, Tianjin, China, in 2010. She is currently pursuing the M.S. degree in precision instrument and optoelectronics engineering at Tianjin University, Tianjin, China. Her research interest is optic-fiber sensors research based on Surface Plasmon Resonance technology.

Kexin Xu received the B.S. degree in precision instrument engineering from Harbin University of Science and Technology, Harbin, China, in 1982 and the Ph.D. degree in precision instrument engineering from Tianjin University, Tianjin, China, in 1988. From 1992 to 1999, he was a senior research fellow and team leader for non-invasive glucose measurement techniques in the Laboratory of Basic Technologies, KDK Corporation, Kyoto, Japan. He obtained his professorship from Tianjin University in 2000. From 2002 to 2012, he was the Dean of the College of Precision Instrument and Opto-Electronic Engineering, Tianjin University. He has published more than 60 research articles, 15 US patents and 5 Chinese patents related to non-invasive blood glucose sensing using near infrared spectrum. His research interest includes the design theory of acousto-optic tunable filter and spectroscopic technology, rapid detection of milk ingredients, monitoring of air and flue gas composition, non-invasive glucose monitoring, etc. He has been a fellow of SPIE since 2007 and he has been conference chairman for many international conferences.